Available online at www.sciencedirect.com
ScienceDirect
Trans. Nonferrous Met. Soc. China 35(2025) 1325−1337
Transactions of Nonferrous Metals Society of China
www.tnmsc.cn

Selective flotation of ilmenite from titanaugite under weakly acidic pH conditions using 2-amino-1-propanol as novel depressant

Chuan DAI[1], Pan CHEN[2], Yao-hui YANG[3], Wei SUN[1], Hong-bin WANG[4,5]

1. School of Minerals Processing and Bioengineering, Central South University, Changsha 410083, China;
2. School of Materials Science and Engineering, Sichuan University, Chengdu 610065, China;
3. Institute of Multipurpose Utilization of Mineral Resources, Chinese Academy of Geological Science, Chengdu 610041, China;
4. Pangang Group Design and Research Institute of Mining Industry Co., Ltd., Panzhihua 617063, China;
5. School of Chemical Engineering, Zhengzhou University, Zhengzhou 450000, China

Received 27 September 2023; accepted 17 April 2024

Abstract: The potential of 2-amino-1-propanol (AP) as a novel depressant in selectively floating ilmenite from titanaugite under weakly acidic conditions was investigated. Micro-flotation results show that AP significantly reduces the recovery of titanaugite while having no evident impact on ilmenite flotation. Subsequent bench-scale flotation tests further confirm a remarkable improvement in separation efficiency upon the introduction of AP. Contact angle and adsorption tests reveal a stronger affinity of AP towards the titanaugite surface in comparison to ilmenite. Zeta potential measurements and X-ray photoelectron spectroscopy (XPS) analyses exhibit favorable adsorption characteristics of AP on titanaugite, resulting from a synergy of electrostatic attraction and chemical interaction. In contrast, electrostatic repulsion hinders any significant interaction between AP and the ilmenite surface. These findings highlight the potential of AP as a highly efficient depressant for ilmenite flotation, paving the way for reduced reliance on sulfuric acid in the industry.

Key words: ilmenite; titanaugite; selective flotation; weakly acidic condition; depressant

1 Introduction

Ilmenite ($FeTiO_3$), a crucial mineral in China's commercial titanium production [1,2], is predominantly extracted through a variety of separation methods, including magnetic separation [3−5], gravity separation [6−8], electrostatic separation [7,9], froth flotation [10−15], and their combinations [16]. Among these methods, froth flotation reigns supreme for its efficiency in removing fine gangue minerals. However, the selective flotation of ilmenite from its main coexisting gangue mineral, titanaugite, presents a significant challenge due to their similar surface-active metal ions (Ti^{4+}, Fe^{2+}, Fe^{3+}, Ca^{2+}, and Mg^{2+}) [17]. Traditionally, achieving high TiO_2 concentrate grades relies on sulfuric acid in the flotation process [18]. This acidic environment promotes the dissolution of Ca^{2+} and Mg^{2+} ions from the titanaugite surface, thereby reducing its surface activity and facilitating depression [19]. Although sulfuric acid plays a vital role in ilmenite flotation, its excessive use carries detrimental consequences such as increased collector consumption, lower recoveries, pipe blockages, and equipment corrosion [11]. Therefore, the development of high-performance depressants that minimize the dependence on sulfuric acid has

Corresponding author: Pan CHEN, Tel: +86-13739081721, E-mail: chenpanscu@163.com
DOI: https://doi.org/10.1016/S1003-6326(24)66751-8

become crucial for sustainable and efficient ilmenite processing.

Depressants, such as water glass and sodium hexametaphosphate, alter the surface potential of gangue minerals, thereby reducing the adsorption of collectors and promoting interparticle repulsion [20]. YANG et al [21] adopted acidified water glass, employing a 3:1 molar ratio of water glass to oxalic acid as the depressant for separating ilmenite from olivine, revealing a preferential interaction between the depressant and olivine. Although inorganic depressants are widely used, organic depressants have drawn more attention due to their advantages in effective separation and environmental sustainability. YUAN et al [22] investigated the effects of carboxymethyl cellulose (CMC) on both ilmenite and titanaugite, revealing its chemisorption onto the Fe-active sites of titanaugite. Similarly, MENG et al [23] utilized carboxymethyl starch (CMS) as a depressant in separating ilmenite from titanaugite, finding enhanced chemisorption and hydrogen bonding on titanaugite. These anionic organic depressants achieve hydrophilic depression by forming chemical bonds with active sites such as Ca, Mg, and Al on the surface of gangue minerals. As a consequence, ilmenite is also subject to depression to some extent due to the presence of surface-active metal ions similar to those on titanaugite. To tackle this challenge, a strategic approach using the inherent difference in surface potential between ilmenite and titanaugite shows great promise for achieving selective separation.

Several studies have elucidated the isoelectric point of ilmenite to be within the range of 5.3−6.0 [24], while titanaugite falls within the range of 3.4−4.0 [23]. Thus, under weakly acidic conditions, the surface charge of ilmenite becomes positive, contrasting with the negative surface charge acquired by gangue minerals. This study suggests employing a cationic alcohol amine with a short carbon chain as a selective depressant for gangue minerals. The aim is to utilize the opposite surface potential properties of ilmenite and gangue minerals, enabling the precise adsorption of the organic depressant onto the surface of gangue minerals through electrostatic adsorption.

In this study, 2-amino-1-propanol (AP), one type of alcohol amine, was first used as a depressant for titanaugite in ilmenite flotation. The effect of AP on the flotation performance of ilmenite and titanaugite, using sodium oleate (NaOL) as a collector, was investigated through micro-flotation tests, bench-scale flotation tests, contact angle tests, zeta potential measurements, adsorption tests, and XPS analysis. The main objective of this study is to identify a highly efficient depressant that enables the effective separation of ilmenite from titanaugite while minimizing the reliance on sulfuric acid usage and revealing the interaction mechanism.

2 Experimental

2.1 Materials and reagents

The raw ore was obtained from the Panzhihua Mining Company in Sichuan, China. The multi-element X-ray fluorescence (XRF) analysis of this ore is shown in Table 1. The ore underwent repeated purification processes, including grinding, recleaning on a shaking table, and magnetic separation, to obtain pure minerals of ilmenite and titanaugite. Minerals ranging in size from 38 to 74 μm were selected from the purified samples for subsequent experiments. X-ray diffraction (XRD) analysis, as presented in Fig. 1, confirmed the purity of both ilmenite and titanaugite exceeding 90%.

Sulfuric acid (H_2SO_4), sodium hydroxide (NaOH), sodium oleate (NaOL), sodium silicate (SS), and 2-amino-1-propanol (AP) were sourced from Macklin Chemical Co., Ltd., while diesel fuel was obtained from a local gas station. These chemicals were utilized in the experimental investigation as follows: H_2SO_4 and NaOH served as pH modifiers; NaOL functioned as a collector for ilmenite and titanaugite; SS was the conventional depressant in ilmenite flotation; AP played the role of a depressant specifically for titanaugite during the flotation; and diesel fuel used as a synergistic collector in the bench-scale flotation tests. The

Table 1 Multi-element analysis results of raw ore (wt.%)

TiO_2	TFe	FeO	Fe_2O_3	CaO	MgO	SiO_2	Al_2O_3	S	Others
15.85	16.43	19.21	2.74	7.44	9.80	19.56	7.13	0.69	1.15

molecular structure of AP is shown in Fig. 2. Deionized water with a resistivity of 18.25 MΩ·cm was used throughout the experiments except for bench-scale flotation tests, which employed tap water.

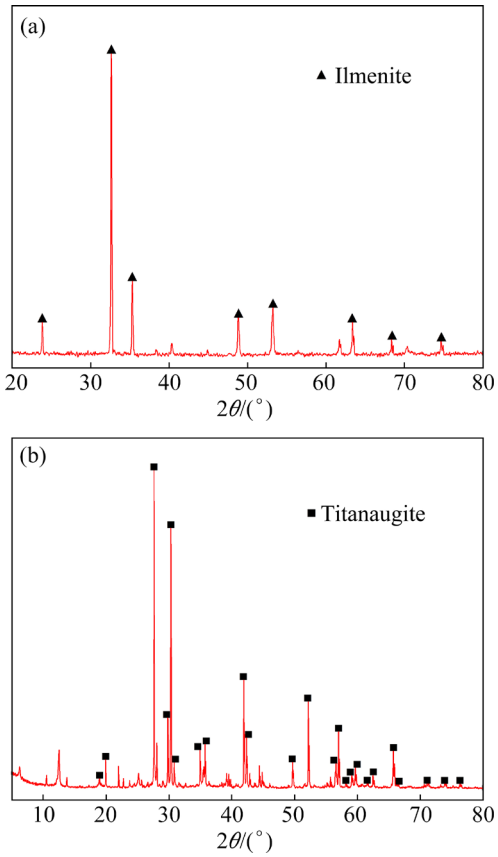

Fig. 1 XRD patterns of purified ilmenite (a) and titanaugite (b)

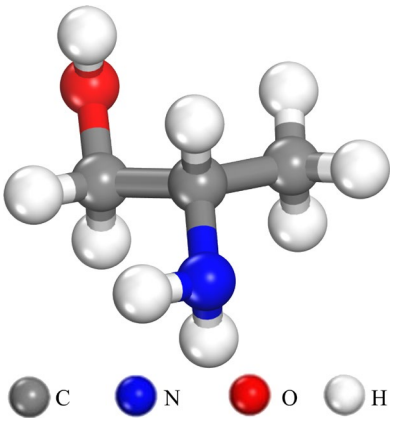

Fig. 2 Molecular structure of AP

2.2 Micro-flotation tests

Micro-flotation tests were conducted using XFG-type equipment operating at a stirring speed of 1700 r/min. 2.0 g of mineral sample was mixed with 40 mL of deionized water. Subsequently, the pH of the system was adjusted using H_2SO_4 for a duration of 3 min. Simultaneously, AP and NaOL were sequentially introduced at 3 min intervals while ensuring continuous agitation. After 3 min of additional stirring, the froth layer was carefully brushed every 10 s to collect the floating minerals. Finally, the resulting foam and sink products were filtered, dried, and weighed to determine the flotation recovery.

2.3 Bench-scale flotation tests

Bench-scale flotation tests were executed following the outlined flowsheet, as depicted in Fig. 3. A 500 g sample was introduced into a 1.0 L XFG-type flotation cell (Jilin Exploration Machinery Factory, China) with an appropriate amount of tap water. Then, H_2SO_4, AP, diesel fuel, and NaOL were added in sequence, and the agitation time of each reagent was 3 min. Air was introduced via the inflation valve, and rougher flotation was conducted for 5 min. Subsequently, the resulting concentrates and tailings were subjected to individual filtration, drying, and weighing processes. The TiO_2 grades of the concentrates and tailings were then analyzed to assess the separation efficiency.

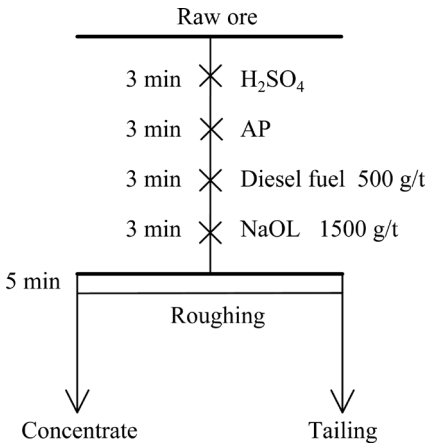

Fig. 3 Flowsheet of bench-scale flotation tests

2.4 Contact angle tests

The contact angles of the minerals were measured using the JC2000A contact angle apparatus. The minerals were treated consistently with the samples used in the flotation tests. After filtration, drying, and compression into smooth lamellar samples, the prepared minerals were carefully positioned in a rectangular glass chamber. The interaction between a liquid droplet and the

sample surface was recorded and analyzed. The contact angles were determined using the established five-point method. Each sample underwent a minimum of three replicate measurements.

2.5 Adsorption tests

The organic carbon content in the solution was quantified using a total organic carbon (TOC) analyzer. 2.0 g of pure ilmenite or titanaugite was used in a pre-filled 40 mL deionized water flotation cell. Subsequently, AP was added to the suspension and stirred for 3 min. The conditioned suspension was then carefully transferred to a 50 mL vial filled with fresh deionized water. Centrifugation at 8000 r/min for 20 min was employed, after which the resulting supernatant was carefully extracted for subsequent TOC analysis. The following formula was utilized to estimate the amount of reagent adsorbed onto ilmenite and titanaugite:

$$\Gamma=(C_0-C)V/m \quad (1)$$

where Γ is the adsorption amount of regents on the mineral surface, mg/g; C_0 and C represent the initial and supernatant concentrations of reagents, respectively, mg/L; V is the supernatant volume, L; m is the mass of mineral, g. The reported values are the average results obtained from three repeated measurements.

2.6 Zeta potential measurements

Zeta potential analysis of the minerals was conducted using a Malvern instrument (Nano ZS90). 20 mg of either pure ilmenite or titanaugite with a particle size of <5 μm (achieved through grinding with an agate mortar) was mixed with 40 mL of a 1.0×10^{-3} mol/L KCl solution. The suspension was conditioned by mechanical stirring for 10 min. The pH was adjusted using H_2SO_4 or NaOH, and then AP or NaOL was added accordingly. Following a settling period of 10 min, supernatant was collected for subsequent zeta potential measurements. The reported results are the average values of three repeated measurements.

2.7 XPS analysis

The procedures utilized for flotation were also employed in preparing samples for X-ray photoelectron spectroscopy (XPS). Initially, the sample was ground to a particle size of <2 μm and weighed 2 g in a 40 mL beaker, followed by the addition of deionized water. After stirring, the pH of the slurry was adjusted to the desired value, and then the reagent was added. The conditioning time was consistent with the flotation tests, after which the samples were collected and dried in a vacuum oven. XPS tests were conducted using a Thermo Fisher ESCALAB 250Xi instrument with an Al K_α X-ray source operating at 1486.6 eV. The high-resolution scans were run with 0.05 eV increments. The obtained XPS spectra were analyzed using Thermo Avantage software, and the spectra were calibrated using the C 1s peak at 284.8eV as the standard.

3 Results and discussion

3.1 Solution chemistry

The influence of pH on flotation performance is evident from the comprehensive depictions in Figs. 4 and 5, which elucidate the surface species distribution of ilmenite and the distribution of NaOL as a function of varying pH.

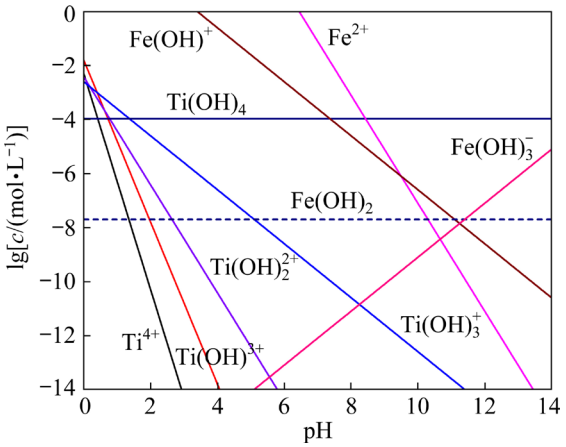

Fig. 4 Surface species on ilmenite as function of pH

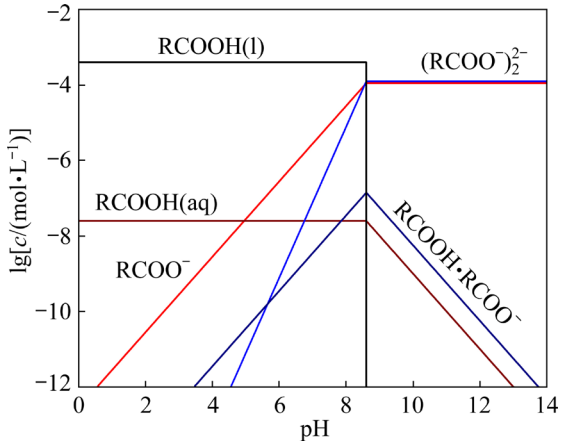

Fig. 5 Distribution of 2.0×10^{-4} mol/L NaOL in solution as function of pH

As depicted in Fig. 4, the Fe^{2+} and Ti^{4+} ions on the ilmenite surface form hydroxyl complex molecules by interacting with OH^- [25]. Under strong acidic conditions (pH less than 3.0), a substantial portion of Fe^{2+} is dissolved from the ilmenite surface, resulting in a predominant presence of Ti^{4+}, $Ti(OH)^{3+}$, and $Ti(OH)_2^{2+}$. However, as the pH increases to a weakly acidic level (pH=5.0−6.0), titanium ions predominantly exist as $Ti(OH)_4$, while ferrous ions primarily adopt the forms of Fe^{2+} and $Fe(OH)^+$. Notably, within this pH range, $Ti(OH)_4$ demonstrates remarkable stability ($K_{Ti(OH)_4}=10^{-58.3}$), where ferrous ions are the sole active sites available for interactions with collector ions. The pH-dependent surface reactivity reveals a notable transition in the distribution of active sites on the ilmenite surface, shifting from Ti-dominated at pH 2.0−3.0 to Fe-dominated at pH 5.0−6.0. This transformation poses a considerable challenge to effectively separating ilmenite from titanaugite.

In the solution, NaOL presents a variety of species, including protonated RCOOH(aq), deprotonated $RCOO^-$, $(RCOO^-)_2^{2-}$, and $RCOOH{\cdot}RCOO^-$ [26]. Within the pH range of 2.0−3.0, the dominant species of NaOL is $RCOO^-$, which effectively interacts with minerals during the flotation process. As the pH increases, the concentration of $RCOO^-$ and $(RCOO^-)_2^{2-}$ also rises. At pH 5.0, the dominant species of NaOL are $RCOO^-$, $(RCOO^-)_2^{2-}$ and $RCOOH{\cdot}RCOO^-$, resulting in a higher abundance of active components on the mineral surfaces. As a result, this enhances the recovery of both ilmenite and titanaugite. Considering the rising pH conditions or the aim to minimize H_2SO_4 consumption, the necessity for a highly efficient depressant becomes crucial in accomplishing the successful separation of ilmenite from titanaugite.

3.2 Micro flotation of single mineral

The influence of pH and depressant AP concentration on the flotation recovery of ilmenite and titanaugite is depicted in Fig. 6.

As shown in Fig. 6(a), the recovery of ilmenite and titanaugite shows an increasing and then decreasing trend without the addition of a depressant. Although ilmenite exhibits higher recovery than titanaugite at the same pH, the recovery difference between the two minerals is merely 6.33% (70.67% for ilmenite and 64.33% for titanaugite) at pH 5.0, posing challenges for effective separation. In contrast, in the presence of AP, the flotation recovery of ilmenite increases from 19.80% to 74.33% with the increase in pH from 3.0 to 5.0, followed by a slight decrease within the pH range of 5.0−9.0. Conversely, the introduction of AP leads to a dramatic decline in titanaugite recovery, dropping from 64.33% to 7.76% at pH 5.0, resulting in a substantial recovery difference of 66.57% between ilmenite and titanaugite. Furthermore, the recovery difference between two minerals reaches 26.50% using the conventional depressant sodium silicate (SS). These results confirm the effectiveness of AP as an exceptional depressant, enabling the selective separation of ilmenite from titanaugite under weak pH conditions.

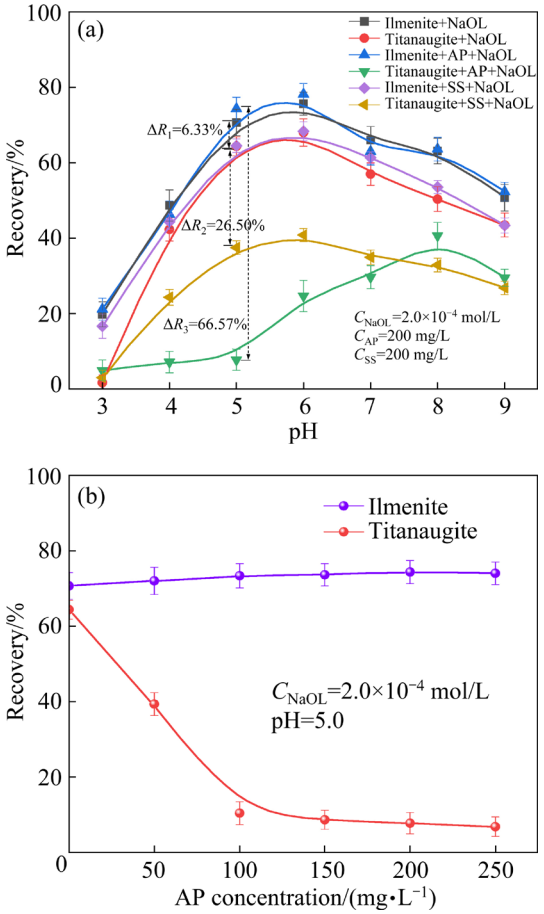

Fig. 6 Effect of pH (a) and AP concentration (b) on flotation recovery of ilmenite and titanaugite

Figure 6(b) illustrates the impact of AP dosage on flotation recovery. The dosage of AP has no significant effect on the flotation recovery of ilmenite. However, titanaugite recovery experiences a substantial decline with the increase in AP

concentration. When the AP dosage surpasses 100 mg/L, the variation in titanaugite recovery becomes negligible, resulting in a remarkable recovery difference above 65% between ilmenite and titanaugite.

3.3 Bench-scale flotation results

Table 2 presents the impact of pulp pH and depressant AP dosage on the flotation performance of the raw ore, with H_2SO_4 serving as the pH modifier.

Table 2 Results of bench-scale flotation under different conditions

Test condition	Product	Yield/%	Grade of TiO_2/%	Recovery of TiO_2/%
pH=2.5, AP: 0 g/t	Concentrate	35.65	29.05	65.34
	Tailing	64.35	8.54	34.66
	Feed	100.00	15.85	100.00
pH=5.0, AP: 0 g/t	Concentrate	52.13	22.36	73.54
	Tailing	47.87	8.76	26.46
	Feed	100.00	15.85	100.00
pH=5.0, AP: 1000 g/t	Concentrate	40.42	29.14	74.31
	Tailing	59.58	6.83	25.69
	Feed	100.00	15.85	100.00

In the absence of AP addition, the increase in pulp pH from 2.5 to 5.0 leads to a significant improvement in concentrate yield, from 35.65% to 52.13%. However, the increase in yield is accompanied by a decrease in concentrate grade, decreasing from 29.05% to 22.36%. This result indicates that reducing the H_2SO_4 dosage weakens titanaugite depression, resulting in a lower TiO_2 grade in the concentrate. In contrast, the introduction of 1000 g/t of AP at a pulp pH of 5.0 results in a significant improvement in separation efficiency, leading to an increase in the concentrate grade to 29.14% and the recovery to 74.31%. Remarkably, this flotation performance demonstrates considerable advancements in grade and recovery, surpassing the results achieved without AP addition.

3.4 Contact angle test results

Figure 7 illustrates the direct reflection of mineral hydrophilicity/hydrophobicity through the contact angle measurements.

Figure 7 illustrates the selective interaction of the depressant AP with ilmenite and titanaugite. Without any reagent, contact angles for ilmenite and titanaugite are recorded as 38.16° and 41.32°, respectively. Upon the introduction of the depressant AP, a slight change is observed in the contact angle of ilmenite, which measures 37.34°. In contrast, the contact angle of titanaugite significantly decreases to 20.15°, confirming the substantial interaction between AP and titanaugite. Furthermore, upon the subsequent addition of NaOL after interaction with AP, the contact angle of ilmenite experiences a notable increase to 65.56°, indicating the limited impact of AP on the adsorption of NaOL onto ilmenite. In contrast, the contact angle of titanaugite increases only to 22.39°, indicating the strong interaction between AP and titanaugite, effectively preventing the adsorption of NaOL on titanaugite.

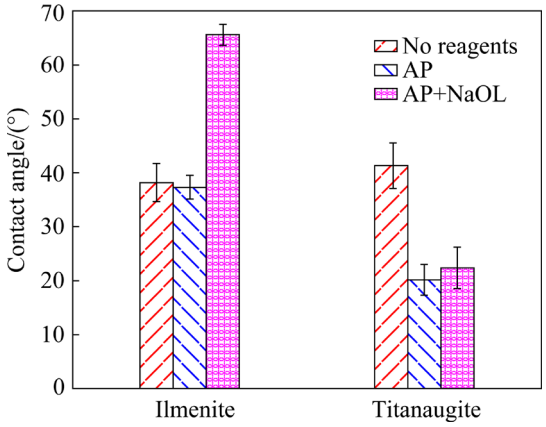

Fig. 7 Contact angles of ilmenite and titanaugite under different conditions (C_{AP}=100 mg/L, and C_{NaOL}=2.0×10^{-4} mol/L)

3.5 Adsorption test results

The micro-flotation tests and contact angle measurements yield insightful findings, revealing that depressant AP exhibits slight adsorption on the ilmenite surface while demonstrating relatively strong adsorption on the titanaugite surface. For a more detailed quantitative evaluation of reagent adsorption on mineral surfaces, adsorption experiments were conducted, as illustrated in Fig. 8.

The data in Fig. 8 indicate that the amount of AP adsorbed on both ilmenite and titanaugite surfaces gradually increases with increasing the dosages of AP. Notably, when the AP dosage is 50 mg/L, the adsorption on the titanaugite surface

reaches 0.65 mg/g, while on the ilmenite surface, it is merely 0.02 mg/g. Beyond an AP dosage of 150 mg/L, there are limited changes in the adsorption amount on both mineral surfaces. Even with an AP dosage of 250 mg/L, the adsorption on ilmenite remains relatively low at 0.12 mg/g, indicating a weak interaction between AP and ilmenite. These results unequivocally demonstrate that under the optimized experimental conditions, AP exhibits selective adsorption on the titanaugite surface, rendering titanaugite hydrophilic and consequently leading to its depression.

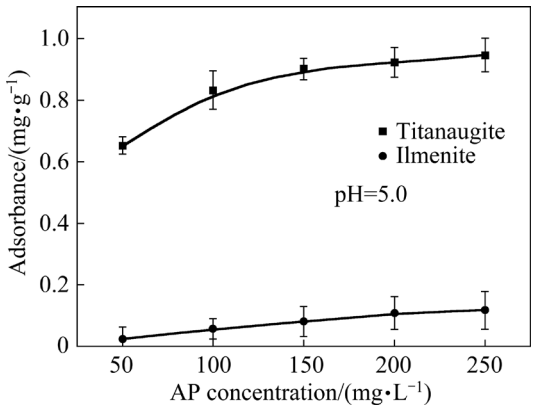

Fig. 8 Effect of AP concentration on absorbance of AP on ilmenite and titanaugite

3.6 Zeta potential and NaOL adsorption density

Figure 9 provides a comprehensive analysis of the interaction mechanism between depressant AP and minerals, as revealed by measuring the zeta potential of ilmenite and titanaugite at different pH values in the absence and presence of reagents. The isoelectric points (IEP) of ilmenite and titanaugite are 5.8 and 3.7, respectively. In the absence of reagents, both ilmenite and titanaugite exhibit gradual decreases in zeta potential as pH increases. At pH 5.0, the positively charged ilmenite and negatively charged titanaugite experience the heterogeneous agglomeration, thereby hindering the selective flotation of ilmenite from titanaugite.

The depressant AP, an amino-containing cationic reagent with a pK_a value of 12.88 reported in the SciFinder database, predominantly exists in the form of AP^+ at pH values below 12.88. Due to the presence of the hydrophilic group (—OH) in its molecular structure, AP also exhibits the properties of a strongly hydrophilic reagent. Upon the introduction of AP, a notable shift in the zeta potential of titanaugite at pH 5.0 is observed. Specifically, the zeta potential of titanaugite shifts by 27.43 mV (from −3.33 to 24.10 mV), while the shift for ilmenite is only 0.96 mV (from 3.77 to 4.73 mV). This difference arises from the positive zeta potential of ilmenite at pH<5.8 (IEP), whereas titanaugite exhibits a negative zeta potential at pH>3.7 (IEP). As a result, electrostatic repulsion exists between the positively charged ilmenite and AP, while electrostatic attraction occurs between AP and the negatively charged titanaugite.

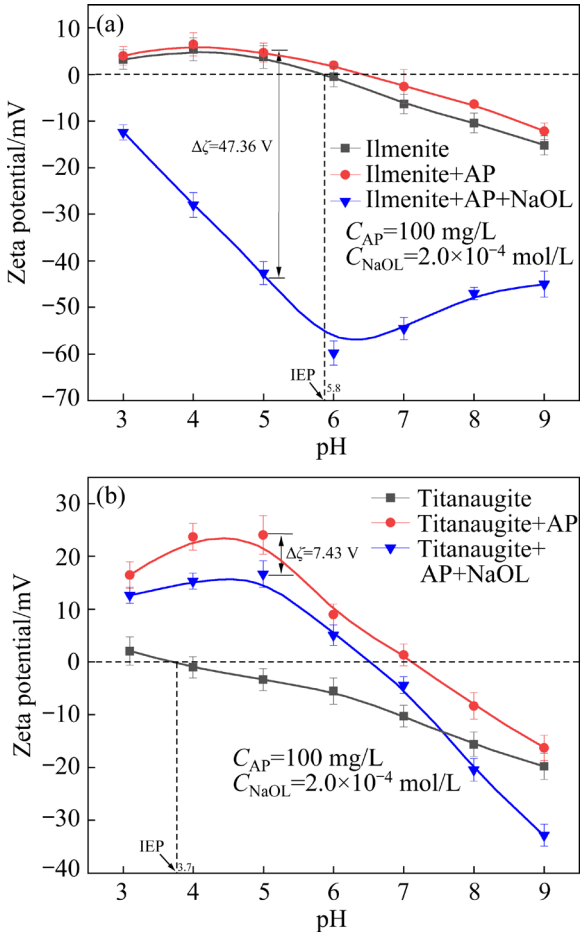

Fig. 9 Zeta potential of ilmenite (a) and titanaugite (b) as function of pH

In the presence of both AP and NaOL, the zeta potential of ilmenite positively shifts by 47.36 mV (from 4.73 to −42.63 mV) at pH 5.0, compared to the addition of only AP. This result demonstrates that the addition of AP has a minimal impact on the adsorption of NaOL onto ilmenite. On the other hand, the zeta potential of titanaugite exhibits a shift of 7.43 mV (from 24.10 to 16.67 mV) at pH 5.0. These findings substantiate that depressant AP does not weaken the adsorption of NaOL on the ilmenite surface. On the contrary, AP exhibits an

enhanced interaction with titanaugite, leading to the effective depression of titanaugite.

During the investigation of NaOL adsorption in the Stern plane, the Stern−Grahame equation can be applied for quantification. The adsorption density of NaOL in the presence of AP can be expressed as follows [27]:

$$\Gamma_s = C\exp\left(\frac{\Delta G_{ads}^0}{RT}\right) \tag{2}$$

where ΔG_{ads}^0 is the standard free energy of adsorption, R is the molar gas constant, and T is the thermodynamic temperature. For most different electrolytes, an approximation is commonly employed, $\Delta G_{ads}^0 = zF\zeta$, where ζ represents the zeta potential approximating the Stern layer potential, z is the valence of the adsorbing ion (z=1 for NaOL), and F corresponds to the Faraday constant. Further studies have demonstrated that the relative adsorption densities of the collector in the Stern plane exhibit a proportionality to exp(Δ|ζ|) when the collector concentration remains constant [26]. Therefore, the equation can be reformulated as

$$\Gamma_s = C\exp\left(\frac{zF\Delta|\zeta|}{RT}\right) = K\exp(\Delta|\zeta|) \tag{3}$$

where K denotes a constant and $\Delta|\zeta| = \zeta_2 - \zeta_1$, and ζ_1 and ζ_2 represent the measured zeta potentials before and after NaOL adsorption, respectively. This difference between the two zeta potential values arises from the strong adsorption of the collector in the Stern plane. Consequently, this difference can be considered a measure of the free energy of adsorption in the Stern plane.

Table 3 displays the relative adsorption densities of NaOL (Γ_s) and the standard free energy of adsorption (ΔG_{ads}^0) for ilmenite and titanaugite at pH 5.0. The assessment of ΔG_{ads}^0 for ilmenite reveals a negative value, signifying the predominant occurrence of chemisorption in the adsorption of NaOL on the ilmenite surface, aligning consistently with prior research findings. Conversely, the evaluation of ΔG_{ads}^0 for titanaugite indicates a positive value, suggesting limited adsorption of NaOL on the titanaugite surface.

3.7 XPS analysis results

XPS analysis was employed to gain deeper insights into the reaction mechanism between AP and minerals. The atomic proportion of elements on the mineral surfaces with or without AP is presented in Table 4.

Table 3 Adsorption densities of NaOL and standard free energy of adsorption at pH 5.0 for AP treated sample

Sample	ζ_1/ mV	ζ_2/ mV	Δ|ζ|/ mV	Γ_s/ (mol·L^{-1})	ΔG_{ads}^0/ kJ
Ilmenite	4.73	−42.63	47.36	*K*exp(0.04736)	−4.11
Titanaugite	24.10	16.67	7.43	*K*exp(0.00743)	1.61

Table 4 Relative contents of elements on surfaces of ilmenite and titanaugite

Sample	Atomic proportion/%						
	C 1s	O 1s	Ti 2p	Fe 2p	Ca 2p	Mg 1s	N 1s
Ilmenite	29.04	56.78	5.44	8.75	−	−	−
Ilmenite+ AP	29.36	56.46	5.73	8.41	−	−	0.04
Titanaugite	26.82	62.62	−	−	4.13	6.43	−
Titanaugite+ AP	29.38	56.84	−	−	4.62	8.16	1.00

As shown in Table 4, the addition of AP to titanaugite results in a significant increase in the atomic proportion of C 1s from 26.82% to 29.38%, as well as a minor increase in N 1s to 1.00%. In contrast, the atomic proportions of elements on the ilmenite surface remain nearly unchanged. To further elucidate the adsorption mechanism between minerals and AP, high-resolution XPS spectra are obtained, as shown in Figs. 10 and 11.

The O 1s peak of ilmenite in Fig. 10(a) is resolved into two peaks at binding energies of 529.84 and 531.52 eV, corresponding to Ti—O and Fe—O bonds, respectively [28]. Following the interaction with depressant AP, the binding energies of Ti—O and Fe—O bonds decrease to 529.79 and 531.44 eV, respectively. The shifts in binding energies are less than the instrumental error of 0.2 eV, which suggests weak interaction between AP and ilmenite. Similar findings are observed in the analysis of the Fe $2p_{3/2}$ and Ti 2p spectra (Figs. 10(b, c)). The characteristic peak for Fe^{2+} at 710.43 eV remains unchanged after treatment with AP. In addition, the peak for Fe^{3+} only slightly shifts from 713.15 to 713.10 eV upon the addition of AP. Similarly, the Ti 2p peak is fitted into two peaks at binding energies of 458.06 and 459.36 eV, which

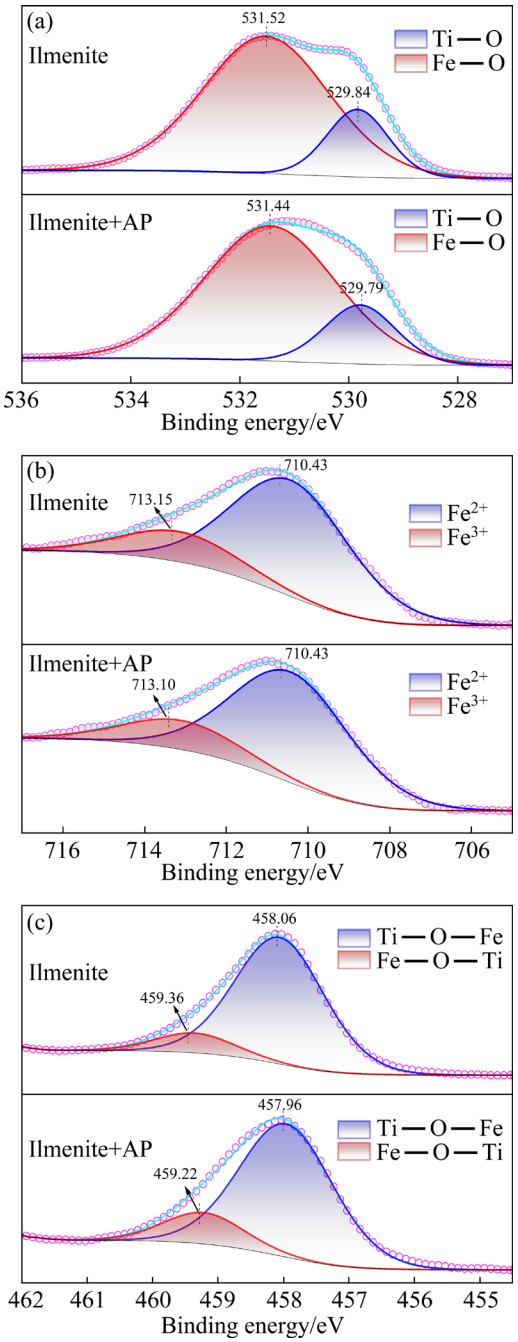

Fig. 10 High-resolution XPS of O 1s (a), Fe $2p_{3/2}$ (b), and Ti 2p (c) on ilmenite surface

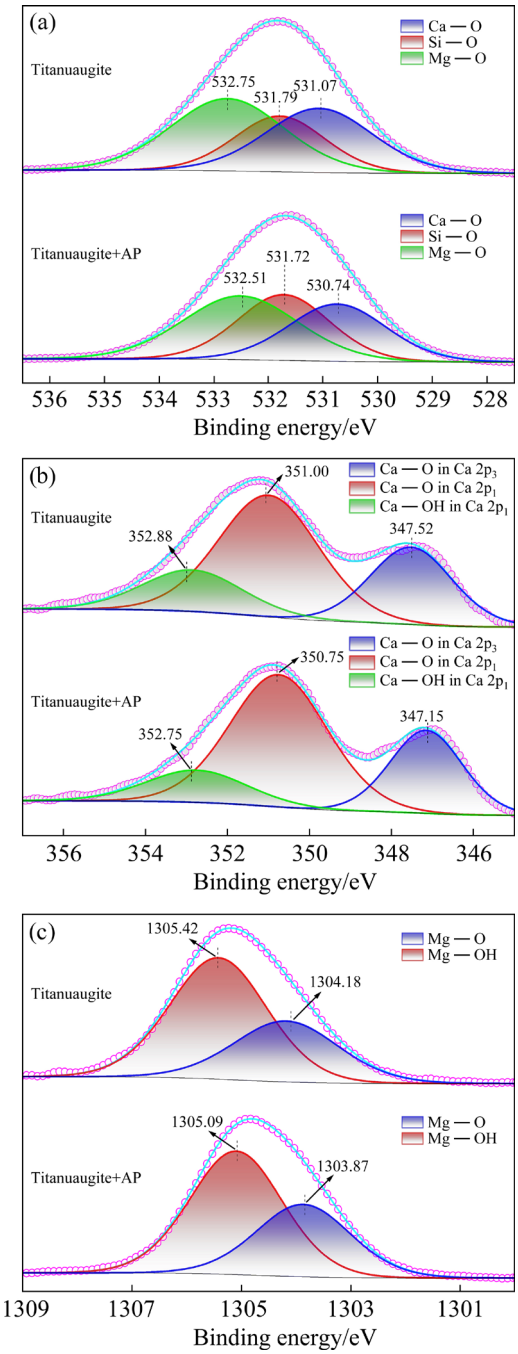

Fig. 11 High-resolution XPS of O 1s (a), Ca 2p (b), and Mg 1s (c) on titanaugite surface

are assigned to the Ti—O—Fe and Ti—O—Ti bonds [29]. After treatment with AP, the binding energies shift to 457.96 and 459.22 eV (a decrease of 0.10 and 0.14 eV). In conclusion, the XPS analysis demonstrates that AP exhibits minimal interaction with ilmenite, consistent with the previously findings.

Figure 11 displays the fitted peaks of titanaugite before and after treatment with AP. In Fig. 11(a), the O 1s peak of untreated titanaugite is resolved into three peaks at 531.07, 531.79 and 532.75 eV, corresponding to Ca—O, Si—O, and Mg — O bonds, respectively [30]. Subsequent treatment with AP induces changes in the binding energies of oxygen species. Specifically, the Ca—O binding energy decreases by 0.33 eV, from 531.07 to 530.74 eV, and the Mg — O binding energy decreases by 0.24 eV, from 532.75 to 532.51 eV. These findings suggest modifications in the chemical states of oxygen species on the titanaugite surface

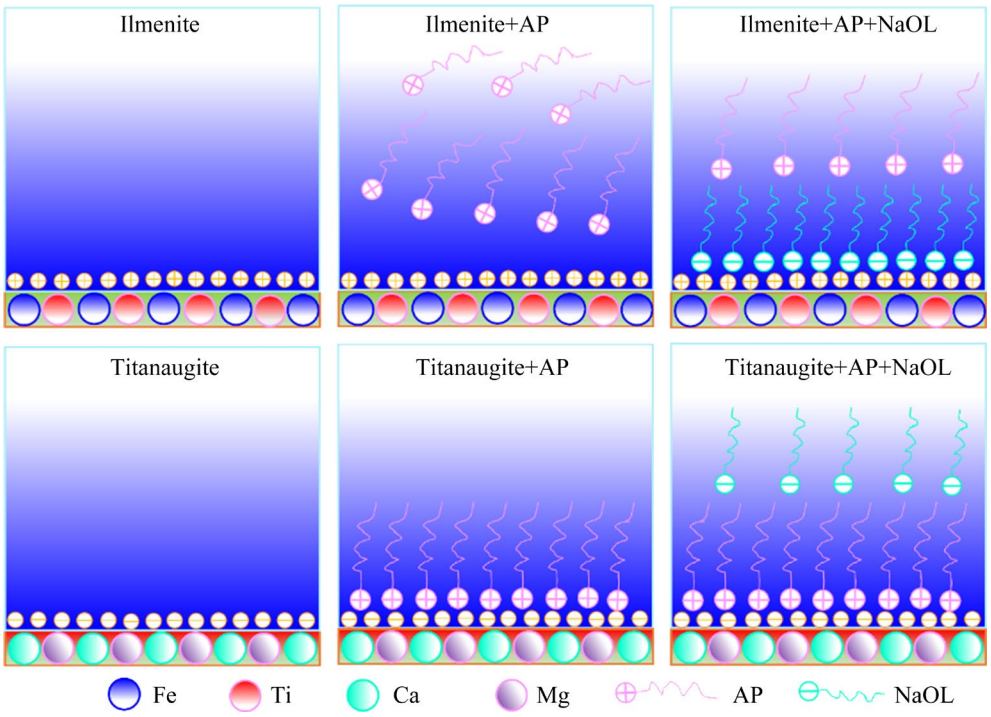

Fig. 12 Potential adsorption mode of AP and NaOL on surfaces of ilmenite and titanaugite

due to the presence of AP. In Fig. 11(b), the Ca 2p peak is resolved into Ca—O and Ca—OH bonds [31]. Following AP treatment, the binding energy of Ca—O in Ca $2p_3$ decreases by 0.37 eV, from 347.52 to 347.15 eV, and in Ca $2p_1$, it decreases by 0.25 eV, from 351.00 to 350.75 eV. These findings indicate a strong interaction with the Ca site on the titanaugite surface due to AP adsorption. Similarly, in Fig. 11(c), the Mg 1s peak of untreated titanaugite is fitted into Mg—O and Mg — OH bonds at 1304.18 and 1305.42 eV, respectively [31]. Following AP treatment, the binding energy of Mg—O decreases by 0.31 eV, from 1304.18 to 1303.87 eV, and that of Mg—OH decreases by 0.43 eV, from 1305.42 to 1305.09 eV. These results indicate a noticeable effect of AP on the Mg site of titanaugite, further demonstrating the strong interaction between AP and the titanaugite surface.

The observed reduction in Ca—O and Mg—O binding energies upon AP treatment can be attributed to the electronegative character of the —OH radical present in AP [32]. This radical likely engages with oxygen atoms on the titanaugite surface, leading to the formation of hydrogen bonds (O — H···O — Ca/Mg). Furthermore, the oxygen atoms within the hydroxyl group possess lone electron pairs that can interact with the metal ions on the titanaugite surface. Consequently, there is an increase in the electron cloud density surrounding Ca—O and Mg—O, resulting in a decrease in binding energy. As the precise nature of the chemical interaction remains elusive, the substantial shift in binding energy suggests a specific and significant interaction, potentially involving a chemical linkage between the functional group of AP and the CaO(OH) or MgO(OH) surface via oxygen atoms [33].

Based on the tests and analyses conducted, a proposed adsorption model illustrating the interaction between AP and NaOL on the mineral surfaces is presented in Fig. 12.

4 Conclusions

(1) AP is proved to be an effective depressant for titanaugite in ilmenite flotation, outperforming the widely used depressant sodium silicate under weakly acidic conditions (pH=5.0).

(2) AP exhibits selective adsorption onto the titanaugite surface, primarily driven by electrostatic interactions and chemisorption with Ca/Mg sites. In contrast, AP displays minimal adsorption onto the ilmenite surface due to electrostatic repulsion.

(3) AP offers a promising approach to reducing the dependence on excessive sulfuric acid usage in ilmenite flotation processes.

CRediT authorship contribution statement

Chuan DAI: Investigation, Formal analysis, Data curation, Validation, Writing − Original draft; **Pan CHEN:** Conceptualization, Methodology, Supervision, Project administration; **Yao-hui YANG:** Funding acquisition, Resources, Visualization; **Wei SUN:** Supervision, Project administration; **Hong-bin WANG:** Funding acquisition, Resources.

Declaration of competing interest

The authors declare that they have no known competing financial interests or personal relationships that could have appeared to influence the work reported in this paper.

Acknowledgments

This work was supported by the National Key Research and Development Program of China (No. 2019YFC1803501), the National Natural Science Foundation of China (No. 52074357), the Natural Science Foundation of Hunan Province, China (No. 2022JJ30713), the Vanadium Titanium Union Foundation, and the Project of Technology Innovation Center for Comprehensive Utilization of Strategic Mineral Resources, Ministry of Natural Resources, China.

References

[1] ZHAI Ji-hua, CHEN Pan, SUN Wei, CHEN Wei, WAN Si. A review of mineral processing of ilmenite by flotation [J]. Minerals Engineering, 2020, 157: 106558. https://doi.org/10.1016/j.mineng.2020.106558.

[2] WU Hou-qin, LUO Li-ping, ZHANG Yong-de, MENG Jin-ping, HUO Xiao-mei, ZHOU Huan, XU Long-hua. New insight into adsorption of novel ternary mixed collector in ilmenite−titanaugite flotation system [J]. Minerals Engineering, 2022, 176: 107319. https://doi.org/10.1016/j.mineng.2020.106558.

[3] MENG Qing-you, DU Yu-sheng, YUAN Zhi-tao, XU Yuan-kai, ZHAO Xuan, LI Li-xia. Study on the mineral characteristics and separation performances of a low-TiO_2 ilmenite [J]. Minerals Engineering, 2022, 179: 107458. https://doi.org/10.1016/j.mineng.2022.107458.

[4] MULABA-BAFUBIANDI A F, MUKENDI-NGALULA D, WAANDERS F B. Ilmenite mineral's recovery from beach sand tailings [J]. Hyperfine Interactions, 2002, 139(1/2/3/4): 485−494. https://doi.org/10.1023/a:1021206324694.

[5] SHEN Shuai-ping, YUAN Zhi-tao, LIU Jiong-tian, MENG Qing-you, HAO Hai-qing. Preconcentration of ultrafine ilmenite ore using a superconducting magnetic separator [J]. Powder Technology, 2020, 360: 1−9.

[6] MAT'ASOVSKY M, SISOL M, MARCIN M, UHLIK P. The possibility of separation of heavy minerals as byproduct of the danube river gravel sand extraction [J]. Minerals, 2022, 12(6): 659. https://doi.org/10.1016/j.powtec.2019.09.074.

[7] REJITH R G, SUNDARARAJAN M. Combined magnetic, electrostatic, and gravity separation techniques for recovering strategic heavy minerals from beach sands [J]. Marine Georesources & Geotechnology, 2018, 36(8): 959−965. https://doi.org/10.1080/1064119x.2017.1403523.

[8] SHIN H Y, CHAE S C, YOO K K. Mineralogy of beach sand in Jumundo, Korea and recovery of heavy minerals using Humphreys spiral concentrator and shaking table followed by magnetic separation process [J]. Geosystem Engineering, 2022, 25(1/2): 1−12. https://doi.org/10.1080/12269328.2022.2074150.

[9] YANG Xing, WANG Hai-feng, PENG Zhen, HAO Juan, ZHANG Guang-wen, XIE Wei-ning, HE Ya-qun. Triboelectric properties of ilmenite and quartz minerals and investigation of triboelectric separation of ilmenite ore [J]. International Journal of Mining Science and Technology, 2018, 28(2): 223−230. https://doi.org/10.1016/j.ijmst.2018.01.003.

[10] DENG Lan-qing, ZHU Liang-di, FEI Ling-yun, MA Xin, DENG Fang, ZUO Rui, HUANG Zhi-qiang, LI Li-qing, XIE Yue-xiang, XIAO Zhi-hong, LIU Ru-kuan. Froth flotation of ilmenite by using the dendritic surfactant 2-decanoylamino-pentanedioic acid [J]. Minerals Engineering, 2021, 165: 106861. https://doi.org/10.1016/j.mineng.2021.106861.

[11] DU Yu-sheng, MENG Qing-you, YUAN Zhi-tao, MA Long-qiu, ZHAO Xuan, XU Yuan-kai. Study on the flotation behavior and mechanism of ilmenite and titanaugite with sodium oleate [J]. Minerals Engineering, 2020, 152: 106366. https://doi.org/10.1016/j.mineng.2020.106366.

[12] MEHDILO A, IRANNAJAD M. Surface modification of ilmenite and its accompanied gangue minerals by thermal pretreatment: Application in flotation process [J]. Transactions of Nonferrous Metals Society of China, 2021, 31(9): 2836−2851. https://doi.org/10.1016/s1003-6326(21)65697-2.

[13] XU Yan-ling, HUANG Kai-hua, LI Hong-qiang, HUANG Wei, LIU Cheng, YANG Si-yuan. Adsorption mechanism of styryl phosphonate ester as collector in ilmenite flotation [J]. Transactions of Nonferrous Metals Society of China, 2022, 32(12): 4088−4098. https://doi.org/10.1016/s1003-6326(22)66080-1.

[14] YANG Yao-hui, XU Long-hua, LIU Ya-chuan, HAN Yue-xin. Flotation separation of ilmenite from titanaugite using mixed collectors [J]. Separation Science and Technology, 2016, 51(11): 1840−1846. https://doi.org/10.1080/01496395.2016.1183678.

[15] ZHU Yang-ge, ZHANG Guo-fan, FENG Qi-ming, YAN Dai-cui, WANG Wei-qing. Effect of surface dissolution on flotation separation of fine ilmenite from titanaugite [J]. Transactions of Nonferrous Metals Society of China, 2011,

21(5): 1149−1154. https://doi.org/10.1016/s1003-6326(11)60835-2.

[16] ZHAI Ji-hua, WANG Hong-bin, CHEN Pan, HU Yue-hua, SUN Wei. Recycling of iron and titanium resources from early tailings: From fundamental work to industrial application [J]. Chemosphere, 2020, 242: 125178. https://doi.org/10.1016/j.chemosphere.2019.125178.

[17] DU Yu-sheng, MENG Qing-you, YUAN Zhi-tao, LIU Zhe, ZHAO Xuan. New insights into the impact of acid surface pretreatment on the flotation of three classified ilmenites [J]. Applied Surface Science, 2022, 599: 153945. https://doi.org/10.1016/j.apsusc.2022.153945.

[18] WANG Sen, XIAO Wei, MA Xiao, LI Jiu-zhou, CHEN Li-juan, YAO Hui. Analysis of the application potential of coffee oil as an ilmenite flotation collector [J]. Minerals, 2019, 9(9): 505. https://doi.org/10.3390/min9090505.

[19] SALMANI NURI O, IRANNAJAD M, MEHDILO A. Effect of surface dissolution on kinetic parameters in flotation of ilmenite from different gangue minerals [J]. Transactions of Nonferrous Metals Society of China, 2019, 29(12): 2615−2626. https://doi.org/10.1016/s1003-6326(19)65168-x.

[20] CAI Jiao-zhong, DENG Jiu-shuai, WANG Liang, HU Ming-zhen, XU Hong-xiang, HOU Xiao-an, WU Bo-zeng, LI Shi-mei. Reagent types and action mechanisms in ilmenite flotation: A review [J]. International Journal of Minerals Metallurgy and Materials, 2022, 29(9): 1656−1669. https://doi.org/10.1007/s12613-021-2380-5

[21] YANG Yao-hui, XU Long-hua, TIAN Jia, LIU Ya-chuan, HAN Yue-xin. Selective flotation of ilmenite from olivine using the acidified water glass as depressant [J]. International Journal of Mineral Processing, 2016, 157: 73−79. https://doi.org/10.1016/j.minpro.2016.10.001.

[22] YUAN Zhi-tao, DU Yu-sheng, MENG Qing-you, ZHANG Chen, XU Yuan-kai, ZHAO Xuan. Adsorption differences of carboxymethyl cellulose depressant on ilmenite and titanaugite [J]. Minerals Engineering, 2021, 166: 106887. https://doi.org/10.1016/j.mineng.2021.106887.

[23] MENG Qing-you, YUAN Zhi-tao, YU Li, XU Yuan-kai, DU Yu-sheng, ZHANG Chen. Selective depression of titanaugite in the ilmenite flotation with carboxymethyl starch [J]. Applied Surface Science, 2018, 440: 955−962. https://doi.org/10.1016/j.apsusc.2018.01.234.

[24] ZHAO Xuan, MENG Qingyou, YUAN Zhi-tao, ZHANG Yun-hai, LI Li-xia. Effect of sodium silicate on the magnetic separation of ilmenite from titanaugite by magnetite selective coating [J]. Powder Technology, 2019, 344: 233−241. https://doi.org/10.1016/j.powtec.2018.12.026.

[25] FAN Xian-feng, WATERS K E, ROWSON N A, PARKER D J. Modification of ilmenite surface chemistry for enhancing surfactants adsorption and bubble attachment [J]. Journal of Colloid and Interface Science, 2009, 329(1): 167−172. https://doi.org/10.1016/j.jcis.2008.09.064.

[26] MEHDILO A, IRANNAJAD M, REZAI B. Effect of crystal chemistry and surface properties on ilmenite flotation behavior [J]. International Journal of Mineral Processing, 2015, 137: 71−81. https://doi.org/10.1016/j.minpro.2015.02.004.

[27] FUERSTENAU D W, SHIBATA J. On using electrokinetics to interpret the flotation and interfacial behavior of manganese dioxide [J]. International Journal of Mineral Processing, 1999, 57: 205−217. https://doi.org/10.1016/s0301-7516(99)00018-6.

[28] MENG Qing-you, YUAN Zhi-tao, YU Li, XU Yuan-kai, DU Yu-sheng. Study on the activation mechanism of lead ions in the flotation of ilmenite using benzyl hydroxamic acid as collector [J]. Journal of Industrial and Engineering Chemistry, 2018, 62: 209−216. https://doi.org/10.1016/j.jiec.2017.12.059.

[29] YANG Si-yuan, XU Yan-ling, LIU Cheng, SORAYA DIALLO A D, LI Chao, LI Hong-qiang. Investigations on the synergistic effect of combined NaOl/SPA collector in ilmenite flotation [J]. Colloids and Surfaces A−Physicochemical and Engineering Aspects, 2021, 628: 127267. https://doi.org/10.1016/j.colsurfa.2021.127267.

[30] YUAN Zhi-tao, ZHAO Xuan, MENG Qing-you, ZHANG Yun-hai, XU Yuan-kai, LI Li-xia. Adsorption mode of sodium citrate for achieving effective flotation separation of ilmenite from titanaugite [J]. Minerals Engineering, 2021, 171: 107086. https://doi.org/10.1016/j.mineng.2021.107086.

[31] ZHAO Xuan, MENG Qing-you, ZHANG Yun-hai, YUAN Zhi-tao, XU Yuan-kai, LI Li-xia. Surface adsorption investigation of dodecylbenzenesulfonate isopropanolamine a novel collector during flotation separation of ilmenite from titanaugite [J]. Minerals Engineering, 2022, 180: 107499. https://doi.org/10.1016/j.mineng.2022.107499.

[32] KASOMO R M, LI Hong-qiang, ZHENG Hui-fang, CHEN Qian, WENG Xiao-qing, MWANGI A D, GE Wu, SONG Shao-xian. Selective flotation of rutile from almandine using sodium carboxymethyl cellulose (Na-CMC) as a depressant [J]. Minerals Engineering, 2020, 157: 106544. https://doi.org/10.1016/j.mineng.2020.106544.

[33] MOREIRA GF, PECANHA E R, MONTE M B M, LEAL FILHO L S, STAVALE F. XPS study on the mechanism of starch-hematite surface chemical complexation [J]. Minerals Engineering, 2017, 110: 96−103. https://doi.org/10.1016/j.mineng.2017.04.014.

弱酸性条件下以 2-氨基-1-丙醇为新型抑制剂浮选分离钛铁矿和钛辉石

戴 川[1]，陈 攀[2]，杨耀辉[3]，孙 伟[1]，王洪彬[4,5]

1. 中南大学 资源加工与生物工程学院，长沙 410083；
2. 四川大学 材料科学与工程学院，成都 610065；
3. 中国地质调查局 矿产综合利用研究所，成都 610041；
4. 攀钢集团矿业有限公司设计研究院， 攀枝花 617063；
5. 郑州大学 化工学院，郑州 450000

摘 要：在弱酸性条件下将 2-氨基-1-丙醇(AP)作为一种新型抑制剂应用于钛铁矿与钛辉石的浮选分离。微浮选试验表明， AP 可以显著降低钛辉石的浮选回收率，而对钛铁矿的浮选影响微弱。随后的中试浮选试验进一步证实引入 AP 可大幅加强分离效率。接触角测试和吸附量测试表明，AP 与钛辉石的作用强于钛铁矿。Zeta 电位测试和 XPS 测试表明，AP 强烈吸附于钛辉石表面是由于静电吸引与化学吸附的共同作用，而 AP 因静电排斥作用难以吸附于钛铁矿表面。与传统的钛铁矿多在强酸性条件下浮选相比，本研究对钛铁矿和钛辉石在弱酸性条件下的分离具有借鉴意义。

关键词：钛铁矿；钛辉石；选择性浮选；弱酸性条件；抑制剂

(Edited by Bing YANG)